Phenotypical Characteristics of *POC1B*-Associated Retinopathy in Japanese Cohort: Cone Dystrophy With Normal Funduscopic Appearance

Shuhei Kameya,[1] Kaoru Fujinami,[2–5] Shinji Ueno,[6] Takaaki Hayashi,[7] Kazuki Kuniyoshi,[8] Ryuichi Ideta,[9] Sachiko Kikuchi,[1,10] Daiki Kubota,[1] Kazutoshi Yoshitake,[11] Satoshi Katagiri,[7] Hiroyuki Sakuramoto,[8] Taro Kominami,[6] Hiroko Terasaki,[6] Lizhu Yang,[2,5] Yu Fujinami-Yokokawa,[2,12,13] Xiao Liu,[2,5,14] Gavin Arno,[2–4,15] Nikolas Pontikos,[2–4] Yozo Miyake,[16] Takeshi Iwata,[11] and Kazushige Tsunoda[2]; for the Japan Eye Genetics Consortium

[1]Department of Ophthalmology, Nippon Medical School Chiba Hokusoh Hospital, Chiba, Japan
[2]Laboratory of Visual Physiology, Division of Vision Research, National Institute of Sensory Organs, National Hospital Organization Tokyo Medical Center, Tokyo, Japan
[3]UCL Institute of Ophthalmology, London, United Kingdom
[4]Moorfields Eye Hospital, London, United Kingdom
[5]Department of Ophthalmology, Keio University School of Medicine, Tokyo, Japan
[6]Department of Ophthalmology, Nagoya University Graduate School of Medicine, Aichi, Japan
[7]Department of Ophthalmology, The Jikei University School of Medicine, Tokyo, Japan
[8]Department of Ophthalmology, Kindai University Faculty of Medicine, Osaka, Japan
[9]IDETA Eye Hospital, Kumamoto City, Kumamoto, Japan
[10]Department of Ophthalmology, Chiba, Japan
[11]Division of Molecular and Cellular Biology, National Institute of Sensory Organs, National Hospital Organization Tokyo Medical Center, Tokyo, Japan
[12]Graduate School of Health Management, Keio University, Kanagawa, Japan
[13]Division of Public Health, Yokokawa Clinic, Osaka, Japan
[14]Southwest Hospital/Southwest Eye Hospital, Third Military Medical University (Army Medical University), Chongqing, China
[15]North East Thames Regional Genetics Service, UCL Great Ormond Street Institute of Child Health, London, United Kingdom
[16]Aichi Medical University, Aichi, Japan

Correspondence: Kazushige Tsunoda, Division of Vision Research, National Institute of Sensory Organs, National Hospital Organization Tokyo Medical Center, 2-5-1 Higashigaoka, Meguro-ku, Tokyo 152-8902, Japan; tsunodakazushige@kankakuki.go.jp.

SKam and KF contributed equally to the work presented here and should therefore be regarded as equivalent authors.

See the appendix for the members of the Japan Eye Genetics Consortium.

Submitted: January 15, 2019
Accepted: June 26, 2019

Citation: Kameya S, Fujinami K, Ueno S, et al. Phenotypical characteristics of *POC1B*-associated retinopathy in Japanese cohort: cone dystrophy with normal funduscopic appearance. *Invest Ophthalmol Vis Sci*. 2019;60:3432–3446. https://doi.org/10.1167/iovs.19-26650

Purpose. Cone/cone-rod dystrophy is a large group of retinal disorders with both phonotypic and genetic heterogeneity. The purpose of this study was to characterize the phenotype of eight patients from seven families harboring *POC1B* mutations in a cohort of the Japan Eye Genetics Consortium (JEGC).

Methods. Whole-exome sequencing with targeted analyses identified homozygous or compound heterozygous mutations of the *POC1B* gene in 7 of 548 families in the JEGC database. Ophthalmologic examinations including the best-corrected visual acuity, perimetry, fundus photography, fundus autofluorescence imaging, optical coherence tomography, and full-field and multifocal electroretinography (ERGs) were performed.

Results. There were four men and four women whose median age at the onset of symptoms was 15.6 years (range, 6–23 years) and that at the time of examination was 40.3 years (range, 22–67 years). The best-corrected visual acuity ranged from −0.08 to 1.52 logMAR units. The funduscopic appearance was normal in all the cases except in one case with faint mottling in the fovea. Optical coherence tomography revealed an absence of the interdigitation zone and blurred ellipsoid zone in the posterior pole, but the foveal structures were preserved in three cases. The full-field photopic ERGs were reduced or extinguished with normal scotopic responses. The central responses of the multifocal ERGs were preserved in two cases. The diagnosis was either generalized cone dystrophy in five cases or cone dystrophy with foveal sparing in three cases.

Conclusions. Generalized or peripheral cone dystrophy with normal funduscopic appearance is the representative phenotype of *POC1B*-associated retinopathy in our cohort.

Keywords: POC1B, cone dystrophy, foveal sparing, normal funduscopic appearance, peripheral cone dystrophy

Cone/cone-rod dystrophy is the name given to a large group of retinal disorders with genetically heterogeneous origin and is characterized by progressive cone dysfunction with or without rod dysfunction. The age of onset, degree of cone/rod dysfunction, and funduscopic appearance are diverse, partly because there are many genetic causes related to this disorder. Representative genotypes related to this disorder involve *GUCY2D*,[1–4] *GUCA1A*,[5–8] *CRX*,[9,10] *RIMS1*,[11] *PROM1*,[12,13] and *PRPH2*[14,15] as autosomal dominant; *ABCA4*[16–19] and *KCNV2*[20–22] as autosomal recessive; and *RPGR*[23,24] as X-linked recessive. It is notable that the clinical features of cone/cone-rod dystrophy are also diverse among the patients having mutations in the same gene or even among patients in the same family. For example, the funduscopic features vary from that of central retinal atrophy, central chorioretinal atrophy, bull's eye appearance, and normal funduscopic appearance, depending on both the genotypes and the individual.[2,7,8,10,11,13,15,16,18,19,21–24]

A normal funduscopic appearance is unusual but not a rare feature of cone dystrophy (COD), and it has been reported in many cases with various genotypes.[10,21,22,24–28] Patients with normal fundus are often misdiagnosed as having optic neuropathy, amblyopia, or nonorganic visual disturbances unless they undergo detailed examinations, including optical coherence tomography (OCT) and electroretinography (ERG). However, there is no report showing that a specific genotype is strongly associated with this funduscopic feature. Thus, to determine the specific genotypes related to normal funduscopic appearance, we have searched for patients with COD that have no apparent funduscopic abnormalities from the genotype-phenotype database of Japan Eye Genetics Consortium (JEGC), and eight cases had putative biallelic mutations in the *POC1B* gene.

POC1B is expressed predominantly in the ciliary region of photoreceptor cells and synapses of the outer plexiform layer of the retina,[29] and homozygous or compound heterozygous mutations in the *POC1B* gene have been reported in cases with COD or cone-rod dystrophy (CORD),[27,29,30] Leber's congenital amaurosis (LCA) with syndromic ciliopathy,[31] and peripheral COD.[28] The funduscopic appearance in these cases varied from normal to peripheral abnormalities and small colobomas with small diameter vessels. However, a detailed clinical and genetic association caused by *POC1B* pathogenic variants has not been published.

Thus, the purpose of this study was to characterize the phenotypical characteristics of eight patients from seven Japanese families harboring *POC1B* mutations in a cohort of the JEGC.

Patients and Methods

The protocol of this study adhered to the tenets of the Declaration of Helsinki and was approved by the Ethics Committee of the participating institutions: National Institute of Sensory Organs (NISO), National Hospital Organization, Tokyo Medical Center; Nippon Medical School Chiba Hokusoh Hospital; Nagoya University Graduate School of Medicine; The Jikei University School of Medicine; Kindai University Faculty of Medicine; Aichi Medical University; and Ideta Eye Hospital. A signed informed consent was obtained from all patients.

Participants

Eight affected patients from seven families who carried multiple *POC1B* variants were studied. The 8 patients were part of the 1035 cases (548 families) in the phenotype-genotype database of the JEGC. The clinical data and results of whole-exome sequencing were available for all the participants. There were 41 cases whose phenotype was "cone/cone-rod dystrophy without apparent funduscopic abnormalities" in the JEGC database, and all of the 8 cases were categorized with this phenotype. The data of two families (families 3 and 6) were partially reported by Kominami et al.[27] and Ito et al.[32]

Clinical Examinations

Comprehensive ophthalmologic examinations were performed on all patients and also on several unaffected family members who were examined for cosegregation analyses (Fig. 1). The clinical evaluations included measurements of the best-corrected visual acuity (BCVA), color vision tests (Ishihara color vision test and the Farnsworth Panel D-15 Color Vision tests), visual field (Goldmann kinetic perimetry and Humphrey Visual Field Analyzer; Carl Zeiss Meditec, Dublin, CA, USA), fundus photography and funduscopy, fundus autofluorescence (FAF) imaging (HRA 2; excitation light, 488 nm; barrier filter, 500 nm; Heidelberg Engineering, Heidelberg, Germany; and 200Tx; excitation light, 532 nm; barrier filter, 570–780 nm; Optos, Dunfermline, United Kingdom), spectral domain optical coherent tomographic (SD-OCT; Cirrus HDOCT, version 6.5-11.0; Carl Zeiss Meditec; and Spectralis; Heidelberg Engineering), and electrophysiologic assessments.

Signal Intensity Profiling of FAF and SD-OCT Images

Signal intensity profiling of the FAF images was performed with a custom-made software (Gray scale profiling version 0.1; modified based on MATLAB 3.0; The MathWorks, Inc., Natick, MA, USA). The gray scales of the obtained FAF images were calculated, and the three-dimensional color tomographic and cross-sectional images based on the gray scales along a selected line were generated. For this study, a horizontal line across the fovea was manually selected to perform the signal intensity profiling of the autofluorescence (AF) density across the fovea. SD-OCT images were obtained, and cross-sectional images based on the gray scales along a selected line were generated according to a published method with custom-made software (Longitudinal profiling version 0.1).[33] The presence of high-intensity lines shown as peaks in the cross-sectional images were assessed for this study.

Electrophysiologic Assessments

For the electrophysiologic assessments, full-field electroretinograms (ERGs) were recorded under both scotopic and photopic conditions in accordance with the protocol of the International Society of Clinical Electrophysiology of Vision.[34] ERGs were recorded with the LE4000 device (Tomey Corporation, Aichi, Japan) or the UTAS device (LKC Technologies, Gaitherburg, MD, USA). Macular function was evaluated by either multifocal ERGs (mfERGs; VERIS Science and VERIS Clinic; EDI, San Mateo, CA, USA) or focal macular ERGs (ER-80; Kowa Company, Tokyo, Japan).[34] All of the clinical data and images were uploaded into the JEGC databank at the NISO, and data quality was confirmed by two of the authors (KF, KT).

Whole-Exome Sequencing and In Silico Molecular Genetic Analysis

Whole-exome sequencing and targeted sequence analyses of the 301 retinal disease-associated genes (including genes of Retnet; https://sph.uth.edu/retnet/, in the public domain) were done according to the published protocol of the NISO.[35] Paired-end sequence library construction and exome capturing were performed at a company (Macrogen, Kyoto, Japan/Gasan-

Investigative Ophthalmology & Visual Science

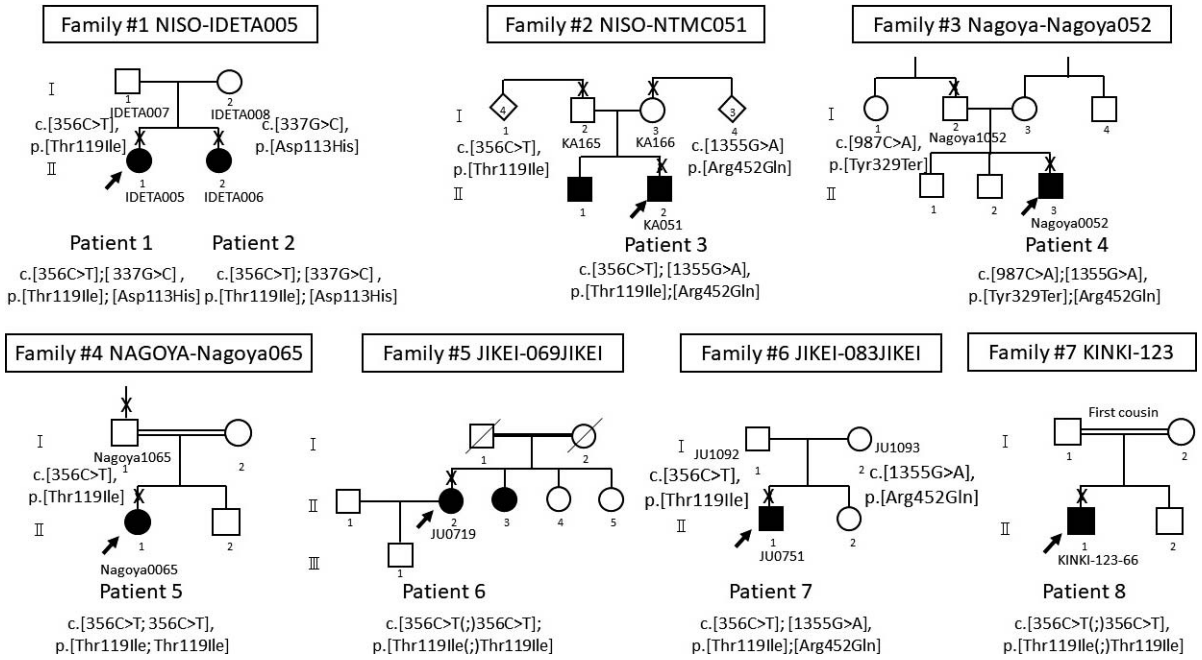

Figure 1. Pedigrees of seven Japanese families with *POC1B*-associated retinopathy. The *solid squares* (men) and *circles* (women) represent the affected patients. Unaffected family members are represented by *clear symbols*. The *slash symbol* indicates deceased individuals. The generation number is shown on the *left*. Patients enrolled in the study are marked by an *arrow*, and the clinically examined individuals are indicated by a *cross*. Detected *POC1B* variants in the affected subjects are shown as follows: patient 1, c.[356C>T];[337G>C], p.[Thr119Ile]; [Asp113His]; patient 2, c.[356C>T]; [337G>C], p.[Thr119Ile]; [Asp113His]; patient 3, c.[356C>T]; [1355G>A], p.[Thr119Ile]; [Arg452Gln; patient 4, c.[987C>A]; [1355G>A], p.[Tyr329Ter]; [Arg452Gln]; patient 5, c.[356C>T; 356C>T], p.[Thr119Ile; Thr119Ile]; patient 6, c.[356C>T(;)356C>T]; p.[Thr119Ile(;)Thr119Ile]; patient 7, c.[356C>T]; [1355G>A], p.[Thr119Ile]; [Arg452Gln]; and patient 8, c.[356C>T(;)356C>T], p.[Thr119Ile(;)Thr119Ile].

dong, South Korea) by the Agilent Bravo automated liquid-handling platform with SureSelect XT Human All Exon kit V3-5 + UTRs kit (Agilent Technologies, Santa Clara, CA, USA). Enriched libraries were sequenced with the Illumina HiSeq 2000/HiSeq 2500 sequencer (San Diego, CA, USA; read length, 2 × 101 bp). Exome pipeline analysis was performed with a customized protocol developed for the Japanese population.[35]

In silico bioinformatic analyses were performed to predict the pathogenicity of all of the identified *POC1B* variants. The identified variants were filtered with allele frequency of less than 1.0% of the Human Genetic Variation Database (http://www.genome.med.kyoto-u.ac.jp/SnpDB/about.html, in the public domain), and 2kJPN (https://ijgvd.megabank.tohoku.ac.jp/download_2kjpn/, in the public domain), which is specific for the Japanese population, and with a total frequency of less than 1.0% of the gnomAD Browser (http://gnomad.broadinstitute.org/, in the public domain). All identified variants were analyzed using three software prediction programs: PolyPhen2 (http://genetics.bwh.harvard.edu/pph/index.html, in the public domain), SIFT (http://sift.jcvi.org/, in the public domain), and mutation taster (http://www.mutationtaster.org/, in the public domain). Conservation in the positions of the identified variants was evaluated with primate PhyloP and phastCons scores provided by University of California-Santa Cruz based on the human genome 19 coordinates (http://genome.ucsc.edu/cgi-bin/hgTrackUi?db=hg19&g=cons46way, in the public domain).

Direct Sequencing

The *POC1B* variants identified by exome sequencing and targeted analysis were further confirmed by direct sequencing of all family members. The identified regions were amplified by polymerase chain reaction (PCR) using primers synthesized by Greiner Bio-One (Tokyo, Japan). The PCR products were purified (ExoSAP-IT; USB Corp., Cleveland, OH, USA) and were used as the template for sequencing. Both strands were sequenced by an automated sequencer (Bio Matrix Research, Chiba, Japan).

Overall, the pathogenicity prediction of all variants, confirmed by direct sequencing, were classified based on the American College of Medical Genetics (ACMG) standards and guidelines.[36]

Results

Whole-exome sequencing with targeted analysis identified homozygous or compound heterozygous mutations of the *POC1B* gene in 8 out of 1035 cases (7 of 548 families) in the JEGC database (Fig. 1).

Demographics, Color Vision Defect, and Visual Fields

The phenotypic findings are shown in Table 1 and 2. There were four women and four men. The median age at the initial examination was 40.3 years with a range of 22 to 67 years, and the median age at the onset of symptoms was 15.6 years with a range of 6 to 23 years. Seven out of eight patients complained of photophobia (88%) as an initial symptom. The BCVA ranged from −0.08 to 1.52 logMAR units. There were no systemic abnormalities described in the reports of all patients.

The results of the Ishihara color vision tests were obtained from 10 eyes of 5 patients (Table 1, 2). Eight eyes of four patients (8/10, 80%) were deficient and the five eyes of three patients could not read any plate including the 1st plate. Therefore, these eyes could not be evaluated by Ishihara color

Table 1. Summary of Clinical Findings 1

Family No.	Patient ID	Age, y	Onset, y	Chief Complaint		LogMAR BCVA		Color Vision	
				1st	2nd	OD	OS	Ishihara	Panel D-15
1	1-II:1 (Patient 1)	35	21	Reduced visual acuity	Photophobia	0.05	0.15	Deficient (readable only the 1st plate, OD; unreadable including the 1st plate, OS)	Fail
1	1-II:2 (Patient 2)	31	10	Photophobia	Reduced visual acuity	1	1	N/A	N/A
2	2-II:1 (Patient 3)	47	22	Photophobia	Reduced visual acuity	0.7	0.7	Deficient (readable only the 1st plate, OU)	Fail
3	3-II:3 (Patient 4)	22	6	Photophobia	Reduced visual acuity	0.7	0.5	Deficient (unreadable including the 1st plate, OU)	Fail
4	4-II:1 (Patient 5)	40	6	Photophobia	Reduced visual acuity	1	1	N/A	Fail
5	5-II:2 (Patient 6)	67	20	Reduced visual acuity		1.52	1.52	Deficient (unreadable including the 1st plate, OU)	Fail
6	6-II:1 (Patient 7)	34	23	Photophobia		−0.08	−0.08	Normal	Pass
7	7-II:1 (Patient 8)	46	17	Photophobia	Color vision abnormality	0.05	0.05	N/A	Fail

ID, identification; OD, right eye; OS, left eye; OU, both eyes; N/A, not available.

vision test (OD of patient 1 and OU of patients 4 and 6). Three eyes of two patients could read only the 1st plate (OS of patient 1 and OU of patient 3). Two eyes of one patient were normal and identified all plates correctly (2/10, 20%). Panel D-15 was performed in seven patients (Table 1, 2; Supplementary Fig. S4). The results of six patients (6/7, 85.7%) were classified as fail. The results of patient 3, 4, 5, and 6 showed many confusion lines between the deutan and tritan axes or along the tritan axes. The results of patients 1 and 8 were fail with two crossings. Two eyes of one patient passed the test (2/14,

Table 2. Summary of Clinical Findings 2

Patient ID	Visual Field	Fundus	FAF	OCT	Full-Field ERG		mfERG/FMERG
					Cone	Rod	
1-II:1 (Patient 1)	Paracentral scotoma, OD Central scotoma, OS (GP)	Normal	N/A	IZ loss, EZ blurring, OU; foveal sparing, OU	Severely reduced	Normal	Preserved central response, OU (mfERG)
1-II:2 (Patient 2)	Central scotoma within 30 degree (GP)	Normal	N/A	IZ loss, EZ blurring, OU	Severely reduced	Normal	Extinguished, OU (mfERG)
2-II:1 (Patient 3)	Central scotoma within 30 degree (GP/HFA)	Small faint spot in the fovea	Foveal hyper AF, OD Normal, OS	IZ loss, EZ blurring, OU	Severely reduced	Normal	Extinguished, OU (FMERG)
3-II:3 (Patient 4)	Central scotoma (GP)	Normal	Foveal hyper AF, OU	IZ loss, EZ blurring, OU	Extinguished	Normal	N/A
4-II:1 (Patient 5)	Central scotoma and perioheral constriction (GP)	Normal	Normal, OU	IZ loss, EZ blurring, OU	Extinguished	Normal	N/A
5-II:2 (Patient 6)	Central scotoma (GP)	Normal	Parafoveal hyper AF, OU	IZ loss, EZ loss, OU	Extinguished	Normal	Extinguished, OU (FMERG)
6-II:1 (Patient 7)	Paracentral scotoma within 20 degree with preserved central sensitivity (GP/HFA)	Normal	Normal, OU	IZ loss, EZ blurring, OU; foveal sparing, OU	Severely reduced	Normal	Preserved central response, OU (mfERG)
7-II:1 (Patient 8)	Paracentral scotoma within 20 degree with preserved central sensitivity (GP/HFA)	Normal	Normal, OU	IZ loss, EZ blurring, OU; foveal sparing, OU	Extinguished	Normal	Extinguished, OU (mfERG)

FAF, fundus autofluorescence; FMERG, focal macular ERG; GP, Goldmann kinetic perimetry; HFA, Humphry static field analyzer; mfERG, multifocal ERG.

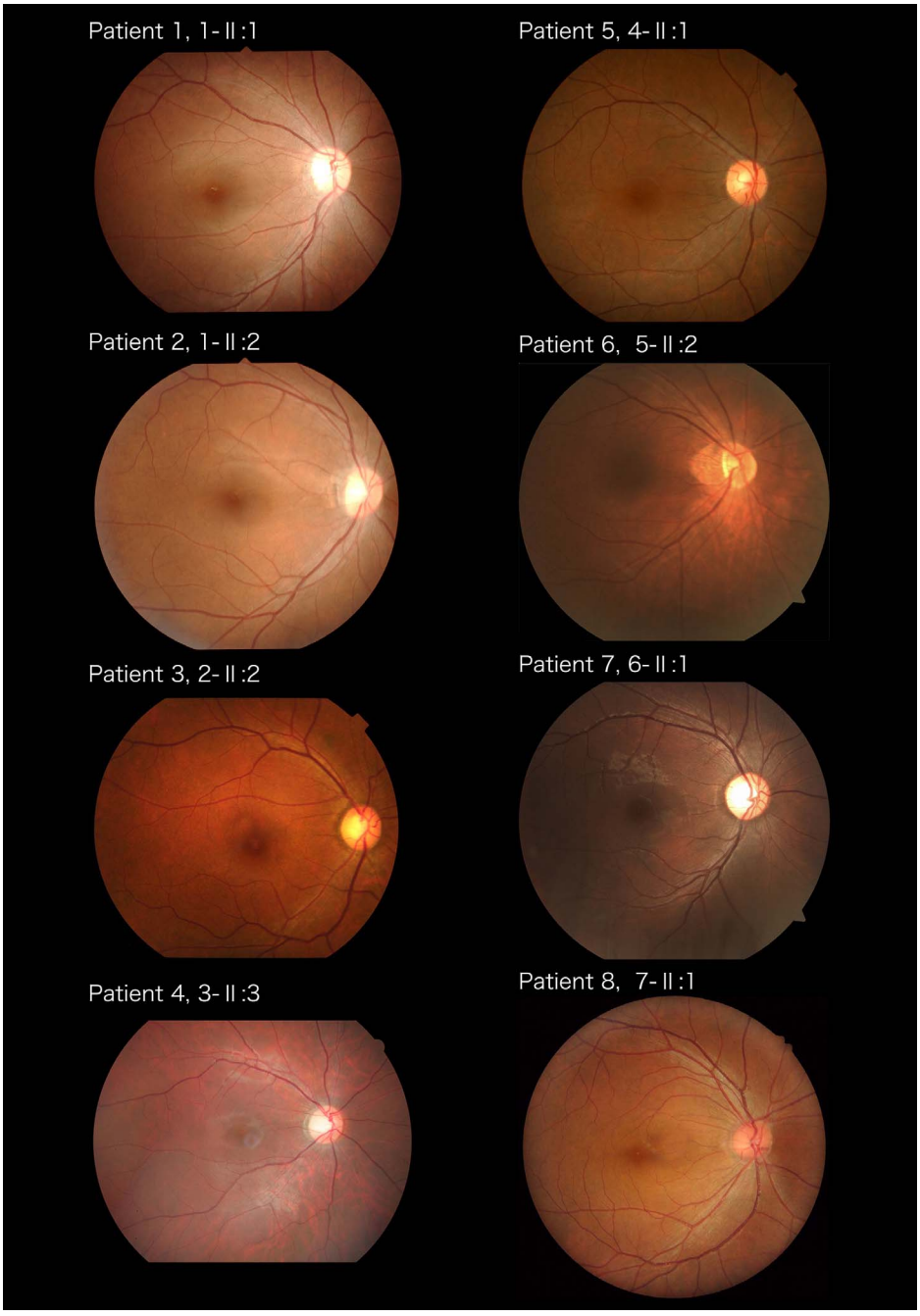

Figure 2. Fundus photographs of all *POC1B*-associated retinopathy patients. Fundus photographs of the right eyes of all patients with *POC1B*-associated retinopathy. No marked abnormalities are present in all of the eyes except for patient 3 (2-II:1) who showed small and faint RPE mottling in the fovea bilaterally

14%). The visual field examinations showed a central scotoma in 11 eyes in 6 patients (11/16, 69%). Patient 3 had a central scotoma by Humphrey Visual Field Analyzer. A paracentral scotoma was found in five eyes of three patients (5/16, 31%).

Fundus and FAF Images

The findings of the funduscopic examinations were normal in all of the eyes except in patient 2-II:1 who showed small and faint retinal pigment epithelial (RPE) mottling in the fovea bilaterally (14/16, 87.5%) (Fig. 2). FAF images were obtained from 12 eyes of 6 patients and signal intensity profiling of gray scales was performed on these 12 images. (Tables 1, 2; Fig. 3; Supplementary Fig. S1). An area of high AF signal was observed in three eyes (patient 3 and 4; 3/12, 25.0%; Table 1, 2; Fig. 3), which was demonstrated as a peak of intensity at the foveola by the gray scale analysis (Supplementary Fig. S1). A band of high AF signal was found surrounding the fovea in two eyes (patient 6; 2/12, 16.7%; Fig. 3). This was seen as a band of slightly increased AF signaling between the fovea and the disc. Although this was a qualitative analysis, the FAF images were seen as hyper-AF in or around the fovea in five eyes of three cases (5/12, 41.7%; Fig. 3, Supplementary Fig. S1). No particular AF abnormalities were detected in seven eyes (7/12, 58.3%; Fig. 3, Supplementary Fig. S1). We compared the

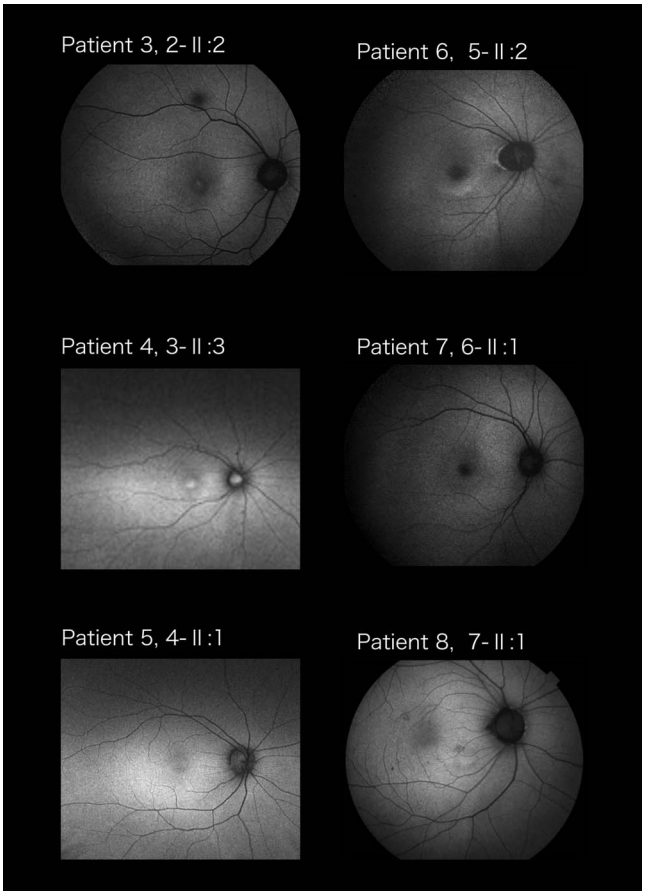

Figure 3. FAF images of six patients with *POC1B*-associated retinopathy (patients 3–8). FAF images of the right eyes of six patients with *POC1B*-associated retinopathy showing an area of high AF signal in patients 3 and 4. A band of high AF signal surrounding the fovea was found in patient 6. No particular AF abnormalities were noted in the other three patients.

feature of cross-sectional images of gray scale profiling obtained from normal controls, *CRX*-retinopathy, and our patients with pathogenic *POC1B* variants. The profile of the eye with *CRX*-retinopathy showed a wider peak of hyporeflectivity as confirmed by the FAF image (Supplementary Fig. S1). However, our patients had a narrower peak of hyporeflectivity similar to that of normal controls.

SD-OCT Images

Signal intensity profiling of the two hyperreflective lines (ellipsoid zone [EZ] and interdigitation zone [IZ]) was performed for the 16 SD-OCT images (Fig. 4; Supplementary Fig. S2). The absence of the IZ and blurred EZ at the posterior polar region was observed in all the eyes (16/16) (Fig. 4), although the EZ of patient 1 and the EZ and IZ of patients 7 and 8 were relatively preserved in a narrow region of fovea as foveal sparing (6/16, 37.5%; shown as asterisks in Fig. 4; Supplementary Fig. S2). In patient 6, the EZ was completely absent bilaterally in the fovea. RPE layer was preserved in all of the eyes (16/16, 100%; Fig. 4; Supplementary Fig. S2).

Electrophysiologic Findings

The cone responses of the full-field ERGs were severely reduced or extinguished in all the eyes (16/16, 100%; Table 1, 2; Fig. 5). The rod responses were normal in all eyes (16/16, 100%; Fig. 5). The mfERGs were preserved in the central fields in four eyes of the two cases tested (4/12, 33%; Table 1, 2; Supplementary Fig. S3), and the others were extinguished in the macular region (8/12, 67%; Table 1, 2).

The clinical diagnosis was either generalized COD in 10 eyes of 5 cases or COD with foveal sparing (i.e., peripheral COD, in 6 eyes of 3 cases).

POC1B Variants

Four possible pathogenic variants were identified: c.337G>C, p.Asp113His; c.356C>T, p.Thr119Ile; c.987C>A, p.Tyr329Ter; and c.1355G>A, p.Arg452Gln (Table 3, 4). Of these variants, Tyr329Ter is a nonsense variant and the others are missense variants. The minor allelic frequency of the four variants was less than 0.2% in two Japanese-specific databases and less than 0.03% in all ethnicities in the gnomAD database (Table 3, 4). The results of three prediction programs indicated that all missense variants were deleterious, probably damaging, and disease causing (Table 3, 4). Two missense variants, Asp113His and Thr119Ile, were located within a WD40 domain, which is critical for proper *POC1B* function (Fig. 6). A missense variant, Arg452Gln, was located at the same position as a reported pathogenic mutation, although the reported mutation was a nonsense mutation (Fig. 6). The conservation score of all missense variants was more than 3.0 in PhyloP, which is relatively high, and mutated amino acids in these variants were well conserved in the homologues of *POC1B* in other species (Table 3, 4; Fig. 7).

Pedigree analyses of families with *POC1B* variants revealed that these four variants were well cosegregated (Fig. 1). Direct sequencing of the four variants detected by whole-exome analysis was performed, and the variants were verified. According to the American College of Medical Genetics standards and guidelines, the *POC1B* variants were considered to be pathogenic, likely pathogenic, or of uncertain significance (Tables 3–5).

Discussion

The proteome of the centriole 1B gene (*POC1B*; OMIM 614784) is one of the two POC1 homologs that function together as a highly conserved core centriole and basal body component.[37] The POC1B protein is localized to centrioles and appear to play roles in centriole duplication and/or maintenance and functions together with POC1A.[38,39] The WD40 repeat domain containing the cartwheel protein Poc1 is required for the structural maintenance of centrioles in *Tetrahymena thermophila*.[37] A knockdown of *poc1b* in zebrafish causes ciliary defects and morphologic phenotypes consistent with human ciliopathies.[37] A morpholino oligomer knockdown of poc1b translation in zebrafish resulted in a dose-dependent small-eye phenotype, impaired optokinetic responses, and decreased length of the photoreceptor outer segments.[40] These findings suggested that poc1b is required for the normal development and ciliogenesis of the retinal photoreceptor sensory cilia.[40]

Homozygous or compound heterozygous mutations of the *POC1B* gene in three Turkish patients and a Dutch subject with COD and CORD were reported in 2014.[29] The three mutations were located in a highly conserved residue within the WD40 domain. This domain is associated with a wide variety of functions, including adaptor/regulatory modules in signal transduction, pre-mRNA processing, and cytoskeleton assembly. WD40 typically contains a GH dipeptide, 11 to 24 residues from its N terminus and a WD dipeptide at its C terminus of 40 residues long, hence the name WD40. Clinical and genetic

Investigative Ophthalmology & Visual Science

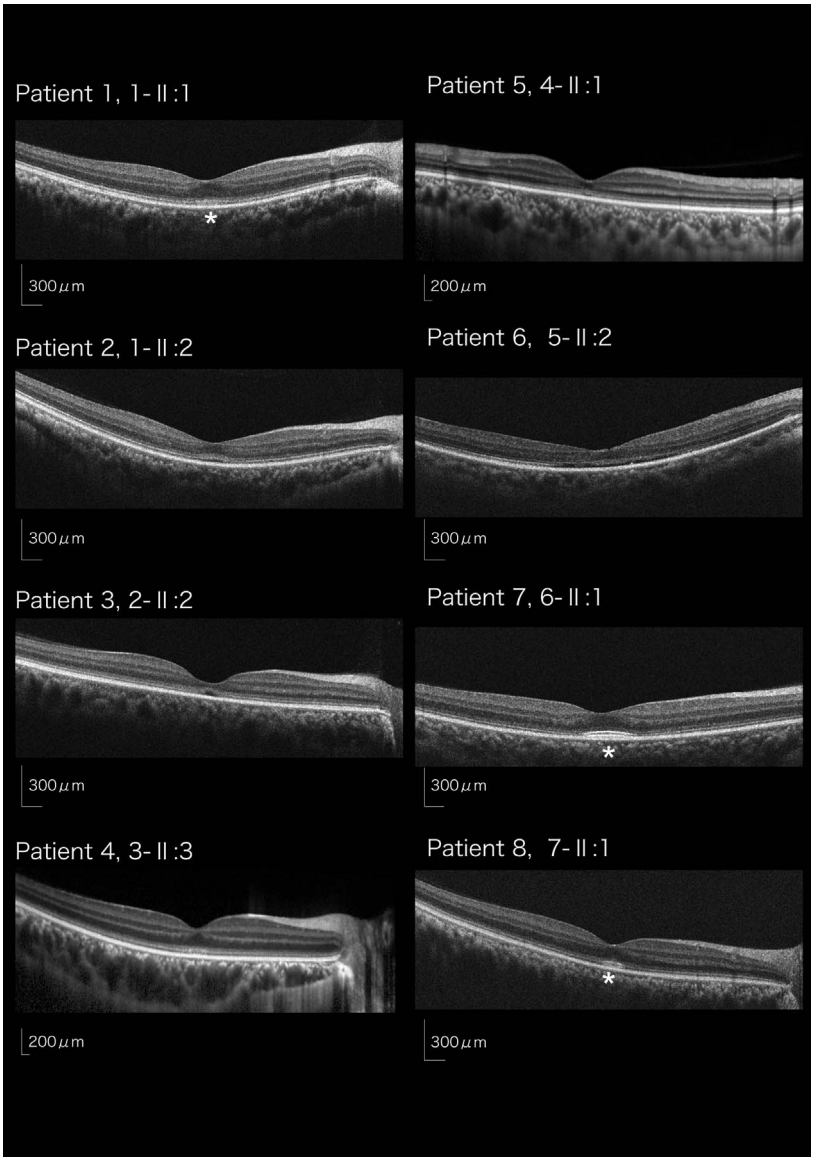

Figure 4. SD-OCT images of all *POC1B*-associated retinopathy patients. SD-OCT images of the right eyes of all patients with *POC1B*-associated retinopathy are shown. The absence of the IZ and blurred EZ at the wide posterior pole region in all the eyes can be seen, although the EZ of patient 1 and both the EZ and IZ of patients 7 and 8 were relatively preserved in a narrow region of the fovea as foveal sparing (shown as *asterisks*). In patient 6 (5-II:2), the EZ was complete absent bilaterally in the macular region. The RPE layer is preserved in all of the eyes.

findings of four affected subjects in a consanguineous Turkish family with CORD were also reported by Durlu et al.[30] in 2014. The recurrent variant c.317G>C, p.Arg106Pro was identified in an Iraqi patient with a severe syndromic retinal ciliopathy in a consanguineous family.[31]

Thus far, only 11 patients from 6 families with biallelic *POC1B* variants have been reported to have retinal abnormalities except in the Japanese patients (Table 6).[27–31,33] We have presented eight Japanese patients from seven families. According to previous reports, a wide variety of phenotypes were observed: one case of LCA, seven cases of CORD, and three cases of COD. The funduscopic appearance was normal in the two Turkish cases and one Chinese case, whereas the other eight cases were reported to have apparent funduscopic abnormalities either in the peripheral retina or in the macular area. On the other hand, all eight cases in the Japanese cohort were diagnosed with COD with preserved rod function (Table 6), and funduscopic examination did not reveal any abnormalities except one case with minimal RPE changes in the fovea (Fig. 2).

The FAF images showed hyper-AF in or around the fovea in five eyes of three cases (Table 1, 2; Fig. 4; Supplementary Fig. S1). These FAF abnormalities, however, were much less severe than in other macular dystrophies.[2,7,10,11,13,15,17,21,23,24,41–43] Also, a hypo-AF, which indicates long-term RPE dysfunction, was not observed in any of the eyes. By comparing the FAF of a severe case with *CRX*-retinopathy that had severe photoreceptor and RPE degeneration at the macula, we would strongly suggest that patients with *POC1B*-associated retinopathy had never had severe hyporeflectivity, as found in patients with *CRX*-retinopathy. This implies that the primary lesion of our cases was the photoreceptors, and the RPE was not severely damaged even in cases with a long disease course. In fact, SD-OCT did not show any abnormalities in the RPE layer, although a loss of the IZ and blurred EZ in the posterior pole were detected in all patients.

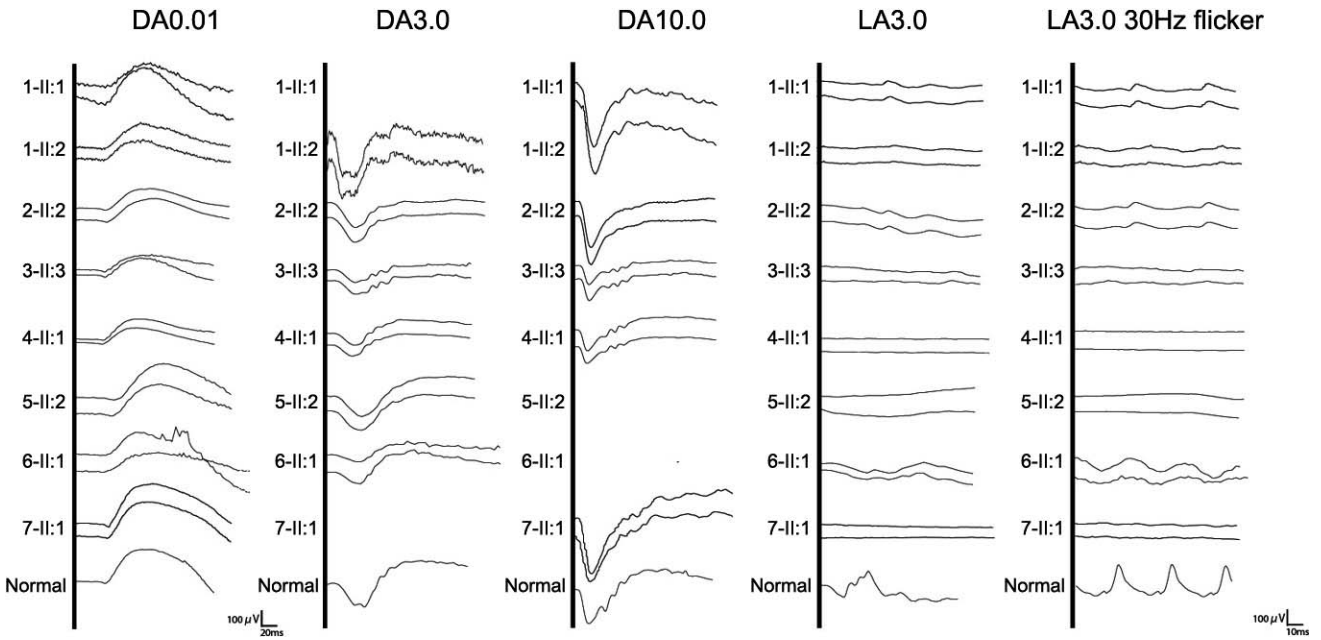

Figure 5. Full-field ERGs of eight *POC1B*-associated retinopathy patients. Full-field ERGs recorded from patients and normal control are shown. The dark-adapted 0.01 (DA 0.01), dark-adapted 3.0 (DA 3.0), dark-adapted 10.0 (DA 10.0), light-adapted 3.0 (LA 3.0), and light-adapted 3.0 flicker (LA 3.0, 30 Hz Flicker) ERGs are shown. The results show extinguished or severe reduction of the cone responses in all patients, although the rod responses are well-preserved.

Table 3. Results of In Silico Genetic Analysis of Four Pathogenic *POC1B** Variants 1

						GnomAD Allele Frequency, %					
Variant ID	HGVS.c	HGVS.p	Position (GRCh 38)	HGVD, %	2kJPN, %	East Asian	South Asian	European (non-Finish)	Latino	African	Total
1	c.337G>C	p.Asp113His	12:89492051	0.0000	0.0000	0.0000	0.0000	0.0000	0.0000	0.0000	0.0000
2	c.356C>T	p.Thr119Ile	12;89492032	0.1652	0.0000	0.0000	0.0000	0.0000	0.0029	0.0000	0.0004
3	c.987C>A	p.Tyr329Ter	12:89466815	0.0000	0.0244	0.0000	0.0000	0.0000	0.0000	0.0000	0.0000
4	c.1355G>A	p.Arg452Gln	12:89421235	0.0000	0.0489	0.0058	0.0067	0.0000	0.0000	0.0207	0.0028

Identified criteria and overall verdict was determined according to the American College of Medical Genetics and Genomics (ACMG) guideline. In silico bioinformatic analyses were performed with three allele frequency databases, three software prediction programs, and conservation scores: HGVD (http://www.genome.med.kyoto-u.ac.jp/SnpDB/about.html, in the public domain), 2kJPN (https://ijgvd.megabank.tohoku.ac.jp/download_2kjpn/, in the public domain), gnomAD Browser (http://gnomad.broadinstitute.org/, in the public domain), PolyPhen2 (http://genetics.bwh.harvard.edu/pph/index.html, in the public domain), SIFT (http://sift.jcvi.org/, in the public domain), and mutation taster (http://www.mutationtaster.org/, in the public domain); primate PhyloP scores and phastCons scores provided by University of California-Santa Cruz (http://genome.ucsc.edu/cgi-bin/hgTrackUi?db=hg19&g=cons46way, in the public domain).

* Reference: ENST00000313546, NM_172240, GRCh38.p7.

Table 4. Results of In Silico Genetic Analysis of Four Pathogenic *POC1B** Variants 2

	Prediction			Conservation Score			ACMG Classification					
Variant ID	SIFT	Polyphen2 HDIV	Mutation Taster	PhyloP	Phast Cons	dbSNP ID	Identified Criteria					Verdict
1	Deleterious	Probably damaging	Disease causing	6.13	1.00	ND		PM2	PM3	PP1	PP3	Likely pathogenic
2	Deleterious	Probably damaging	Disease causing	6.08	1.00	rs1225701102		PM2	PM3	PP1	PP3	Likely pathogenic
3	NA	NA	NA	3.44	1.00	ND	PVS1	PM2			PP3	Pathogenic
4	Deleterious	Probably damaging	Disease causing	4.68	1.00	rs200082142		PM2	PM3		PP3	Uncertain significance

PVS, pathogenic very strong (null variant in a gene where loss of function is a known mechanism of disease); PM2, pathogenic moderate 2 (absent from controls); PM 3, pathogenic moderate 3 (for recessive disorders, detected in trans with a pathogenic variant); PP1, pathogenic supporting 1 (cosegregation with disease in multiple affected family members); PP3, pathogenic moderate 3 (multiple lines of computational evidence support a deleterious effect on the gene or gene product); HGVD, Human Genetic Variation Database; ACMG, American College of Medical Genetics and Genomics.

* Reference: ENST00000313546, NM_172240, GRCh38.p7.

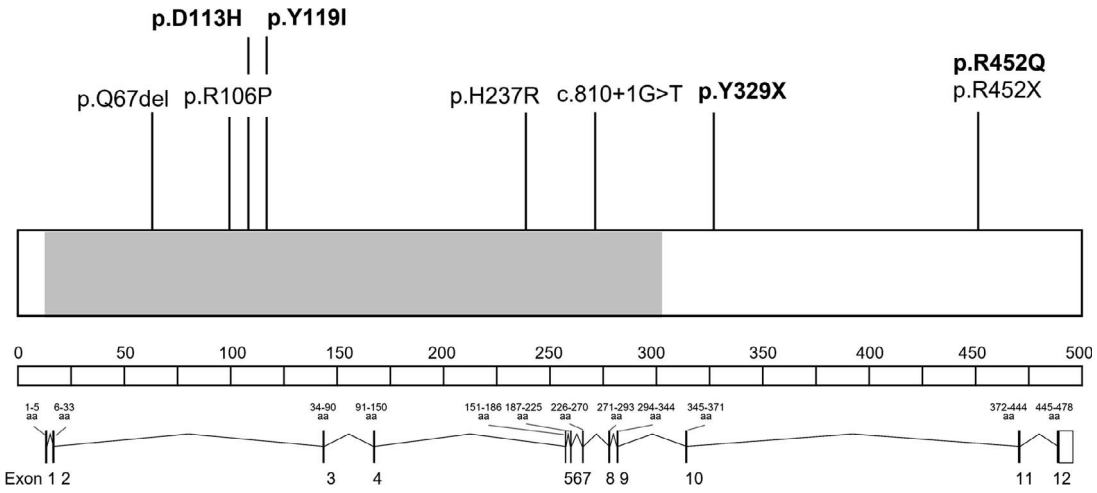

Figure 6. Schematic representation of *POC1B* gene and mutations. The schematic structure of *POC1B* gene are shown. The encoded protein contains seven WD repetitive domains, which are located between amino acids 16 and 307 (highlighted in *gray*). The detailed locations of the seven WD domains are 16–55, 58–99, 101–139, 142–181, 183–223, 226–265, and 268–307 (UniProtKB - Q8TC44 [POC1B_HUMAN]; https://www.uniprot.org/uniprot/Q8TC44, in the public domain). Exon-intron structure and exon numbers are shown under the scheme. Variants in this study and previous reports are shown at the *top* and the variants identified in this study are shown in *bold*.

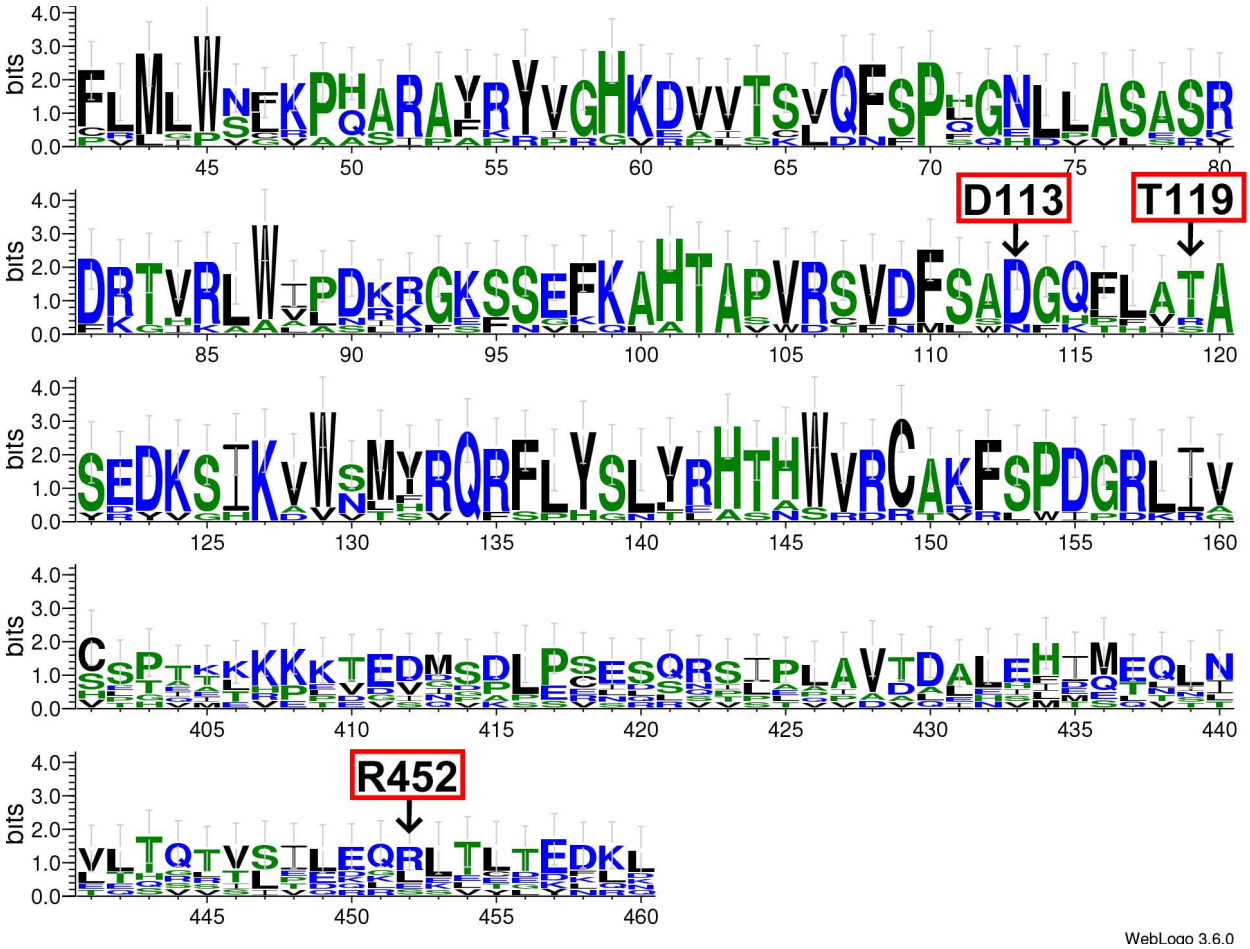

Figure 7. Alignment of *POC1B* family proteins. The result of Weblogo analysis derived from amino acid sequences of POC1B from seven species reported in the NCBI database are shown: *Homo sapiens*, *Mus musculus*, *Xenopus tropicalis*, *Bos taurus*, *Macaca mulatta*, *Canis lupus familiaris*, and *Callithrix jacchus*. Amino acid residues of D113, T119, and R452 in humans are indicated. Well-conserved residues are shown in *larger letters* (WebLogo; https://weblogo.berkeley.edu/logo.cgi in the public domain).

Table 5. Pathogenicity Evaluation of *POC1B* Variants and ACMG Classification in Each Patient

Family No.	Patient ID	Inheritance	Sex	Age, y	Clinical Diagnosis	Consanguinity	HGVS.p	ACMG Classification
1	1-II:1 (Patient 1)	AR	F	38	COD with foveal sparing		D113H	Likely pathogenic
							T119I	Likely pathogenic
1	1-II:2 (Patient 2)	AR	F	34	COD		D113H	Likely pathogenic
							T119I	Likely pathogenic
2	2-II:1 (Patient 3)	AR	M	47	COD		T119I	Likely pathogenic
							R452Q	Uncertain significance
3	3-II:3 (Patient 4)	AR	M	22	COD		Y329X	Pathogenic
							R452Q	Uncertain significance
4	4-II:1 (Patient 5)	AR	F	40	COD	+	T119I	Likely pathogenic
							T119I	Likely pathogenic
5	5-II:2 (Patient 6)	AR	F	67	COD	+	T119I	Likely pathogenic
							T119I	Likely pathogenic
6	6-II:1 (Patient 7)	AR	M	34	COD with foveal sparing		T119I	Likely pathogenic
							R452Q	Uncertain significance
7	7-II:1 (Patient 8)	AR	M	46	COD with foveal sparing	+	T119I	Likely pathogenic
							T119I	Likely pathogenic

AR, autosomal recessive.

It is notable that foveal sparing (i.e., preserved foveal EZ and IZ) was observed in six eyes of three cases (Fig. 4; Supplementary Fig. S2). All of the eyes with foveal sparing had good BCVA between −0.08 and 0.15 logMAR units (Table 1, 2). Among them, four eyes of two cases had preserved mfERGs in the central region (Supplementary Fig. S3).

A foveal sparing was also reported in a Chinese patient with the *POC1B* mutation and was diagnosed with peripheral COD.[28] Peripheral COD was first reported in three Japanese cases of cone dysfunction with preserved macular responses in the ERGs by Kondo et al.[44] These cases had normal funduscopic appearance in both the macula and peripheral retina. The pedigree of one family suggested an autosomal recessive inheritance; however, the causative gene has not been definitively determined. In our six eyes with preserved foveal structures in the OCT images, two eyes did not have preserved central responses in the mfERGs (patient 8; Table 1, 2; Supplementary Fig. S3), although the BVCA was 0.05 logMAR units bilaterally. This may be because the preserved foveal region was too small to evoke normal ERGs, and we suggest that the etiology of our three cases was similar to that reported by Kondo et al.[44]

A sparing of the fovea is commonly observed in different types of macular diseases, such as in *ABCA4*- and *PRPH2*-associated retinopathies,[17,18,43,45–48] mitochondrial retinal dystrophy,[49] macular dystrophy with *CRB1* mutation,[50] and age-related macular degeneration.[51–54] The explanations for the physiologic and anatomic sparing of the fovea have been presented in many publications.[55–63] However, foveal sparing in these macular diseases is usually accompanied by RPE atrophy around the fovea, and the border between the atrophic region and normal fovea is distinct. The foveal sparing in our cases did not show any funduscopic changes because the RPE layer was normally preserved whether the photoreceptor layer is damaged or not (Fig. 2). Thus, the pathologic mechanism for the foveal sparing may differ between the cases with *POC1B* mutations and other macular dystrophies.[17,18,43,45–54] Although the numbers of the eyes with foveal sparing are limited, further investigations to determine whether there is a significant association between the genotype and RPE findings (i.e., the presence or absence of RPE atrophy) in a large cohort with foveal sparing could determine the mechanism of the foveal sparing.

The question then arises on whether the cases with foveal sparing represent an early stage that will progress to a more advanced stage with foveal abnormalities. The BCVA of the left eye of patient 1 deteriorated from 0.15 logMAR units to 0.4 logMAR units after 4 years of follow-up, and the OCT images with the reflectivity profiles also showed that the foveal sparing disappeared during the course; the EZ became blurred and the IZ disappeared at the fovea (Fig. 8, asterisks). The reflectance intensity of the IZ relative to the RPE was 0.82 at 35 years and 0.63 at 39 years. The reflectance intensity of the EZ relative to the RPE was 0.86 at 35 years and 0.77 at 39 years. These findings indicate that the reflectance of both IZ and EZ relative to the RPE were decreased during a follow-up period of 4 years. The changes in the SD-OCT images indicated that foveal sparing is observed during the natural course of the disease process in our cases with *POC1B* mutations and may progress to foveal dysfunction with reduced BCVA with increasing time. Because not all the patients had been followed for a long period of time, we cannot conclude whether the central foveal sparing observed in our patients could be an initial phase of the disorder or a subtype of the phenotypes in the *POC1B*-associated retinopathy. Long-term observations should be able to confirm the natural course of these cases.

The SD-OCT findings of our cases were similar to those of occult macular dystrophy with the *RP1L1* mutation, Miyake's disease, in that both EZ blurring and IZ loss were observed in the affected region without RPE atrophy.[34,64,65] Because both *POC1B* and *RP1L1* are located at the retinal photoreceptor sensory cilia, there is a possibility that the loss of IZ and blurred EZ with preserved RPE are diagnostic markers for retinal ciliopathies. There are, however, other ciliopathies affecting the retina, such as *RPGR*-,[66–68] *RPGRIP1*-,[69–71] *RP1*-[72–74] and *CEP290*-associated retinopathies,[75,76] which commonly lead to an apparent RPE degeneration. The mechanism of why RPE atrophy is less distinct in *POC1B*- and *RP1L1*-associated retinopathy is not clear.

Normal rod function and preserved RPE structures, which are associated with normal funduscopic appearances, are characteristic features in both the Japanese and Chinese cases with *POC1B*-associated retinopathy. On the other hand, the reports of non-Asians identified funduscopic abnormalities in 8 of 10 cases (Table 6).[29–31,41] The phenotypic differences among the different cohorts may arise from either variations in ethnicity or the existence of recurrent R106P variants, which

Table 6. Previously Reported *POC1B* Mutations With Retinal Dystrophies

HGVS.c	HGVS.p	Zygosity	Ethnicity, Cases, *n*	Clinical Diagnosis, *n*	Fundus Appearance	Foveal Sparing	Reference	Year Reported
c.317G>C	p.Arg106Pro	Homozygous	Turkish, 4	4; CRD	2; Normal 2; Peripheral chorioretinal atrophy	(−)	Durlu et al.[30]	2014
c.317G>C	p.Arg106Pro	Homozygous	Turkish, 3	2; COD 1; CRD	3; Peripheral abnormality	(−)	Roosing et al.[29]	2014
c.199_201del, c.810+1G>T	p.Gln67del, p.unknown	Compound heterozygous	Dutch, 1	1; CRD	1; Peripheral abnormality	(−)		
c.317G>C	p.Arg106Pro	Homozygous	Iraqi, 1	1; LCA with syndromic ciliopathy	1; Coloboma (OD) and small vessel diameter (OU)	(−)	Beck et al.[31]	2014
c.317G>C	p.Arg106Pro	Homozygous	German, 1	1; CRD	1; Mild granular irregularities and whitish peripheral flecks	(−)	Birtel et al.[41]	2018
c.710A>G, c.1354C>T	p.His237Arg, p.Arg452X	Compound heterozygous	Chinese, 1	1; COD with foveal sparing	1; Normal	1; (+)	Jin et al.[28]	2018
c.337G>C, c.356C>T, c.987C>A, c.1355G>A,	p.Asp113His, p.Thr119Ile, p.Tyr329Ter, p.Arg452Gln	Homozygous and compound heterozygous	Japanese, 8	5; COD and 3; COD with foveal sparing	7; Normal and 1; Small faint spot in the fovea	3; (+) and 5; (−)	Kominami et al.,[27] This study	2018 partially

were not found in the Japanese or Chinese patients. However, it should be noted that the funduscopic appearances and FAF images of the *POC1B*-associated retinopathy in non-Asian populations were much less severe than those in COD and CORD caused by mutations of other genes.[30,41] A relatively preserved RPE function, which leads to normal funduscopic appearance, may be a common feature of *POC1B*-associated retinopathy in individuals of Asian ethnicities.

Of the 41 cases in the JEGC database registered as cone/cone-rod dystrophy without apparent funduscopic abnormalities, 8 cases with *POC1B*-associated retinopathy were identified, while there were no cases with *POC1B*-associated retinopathy in 161 patients with "macular dystrophy/cone rod dystrophy with apparent funduscopic changes" in the JEGC cohort. This fact implies that *POC1B*-associated retinopathy is a major subset of cases with cone/cone-rod dystrophy.

Our study has a number of limitations. Our data were obtained from the JEGC database for inherited retinal degeneration from all over Japan. The data from patients from multiple institutions were uploaded into the database. However, the examination devices used at the different institutions could have been different. Therefore, detailed quantitative analysis could not be made. More detailed quantitative analyses are needed to resolve this limitation.

The results of Ishihara color vision test showed that five eyes of three patients (patient 1, 4, and 6) could not read any plate including the 1st plate. The results of Panel D-15 of these eyes were fail with two crossings or many confusion lines mainly between the deutan and tritan axes. It is unusual that patients with a BCVA better than 1.0 logMAR units could not identify the 1st plate of the Ishihara color vision test. To address these color vision deficiencies, another detailed color vision assessment such as 100-Hue tests would be needed. The results of Ishihara and Panel D-15 tests of patients 3 and 5 could be considered as behavior of severe red-green deficiency or achromatopsia. There are reports of congenital achromatopsia, which shows similar pattern such as cone dysfunction in the ERG, loss of IZ in the OCT, and D-15 abnormality with confusion lines between deutan and tritan.[77,78] The course of our cases was progressive and was not like that of congenital achromatopsia. However, the relationship between the results of color vision tests and OCT images could not be revealed. In addition, we could not rule out the complications of congenital red-green color deficiency based on the results of color vision tests in this study.

We performed whole-exome sequencing with targeted analysis that could have missed the disorder-causing variants in genes outside of target (301 retinal disease-associated genes) and structural variants including large deletions in the target region. More comprehensive gene screening and analysis by methods such as whole-genome sequencing could help to determine the genetic aberrations of our cohort. We have examined patients with pathogenic *POC1B* variants in a relatively large Japanese cohort, but it is important to note that we have examined only eight patients. The cross-sectional nature of our study did not allow us to draw conclusions regarding the phenotype-genotype correlation of *POC1B* retinopathy. Although several cases had clear onset with notable visual impairment and progression and an evidence of morphologic changes, which suggests the progression of *POC1B*-associated retinopathy, the features and rate of progression were not determined. To address these issues, systematic longitudinal studies incorporating detailed ophthalmologic assessments in large cohort are needed, and they should help determine the mechanisms involved in the development of *POC1B*-associated retinopathy.

In conclusion, the results indicate that a generalized or peripheral COD with normal funduscopic appearance is the

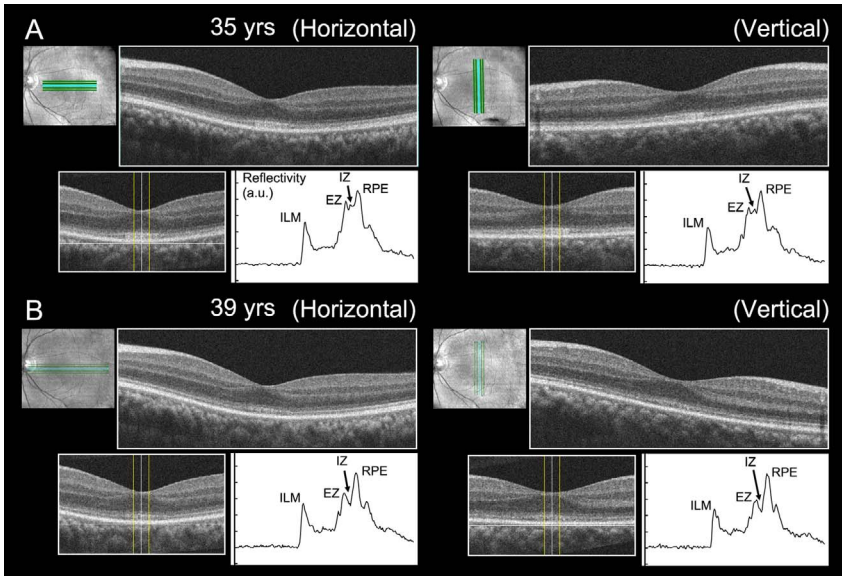

Figure 8. Horizontal and vertical OCT images of the left eye of patient 1 recorded at the age 35 years (**A**) and 39 years (**B**). Longitudinal reflectivity profiles at the fovea are shown *below* the OCT images. EZ and IZ are preserved in the fovea at the age 35 years but they are blurred at the age of 39 years. The reflectivity profiles show small peaks of IZ at the age 35 years but not at 39 years. The reflectance intensity of the IZ relative to the RPE was 0.82 at the age 35 years and 0.63 at the age 39 years. The reflectance intensity of the EZ relative to the RPE was 0.86 at the age 35 years and 0.77 at the age 39 years. The reflectivity was averaged in width as indicated by the *yellow lines*. ILM, internal limiting membrane; a.u., arbitrary unit.

representative phenotype of *POC1B* retinopathy in the Japanese. The characteristic morphologic changes in the photoreceptor layers are similar to those of occult macular dystrophy with the *RP1L1* mutation, which is also one of the retinal ciliopathies and might be a distinctive phenotypic feature to differentiate *POC1B*-associated retinopathy from the other COD or CORD.

Acknowledgments

The authors thank the patients and their families for participation in this study, Kazuki Yamazawa for his expert comments on genetic assessments, and Duco Hamasaki of the Bascom Palmer Eye Institute, University of Miami School of Medicine (Miami, FL, USA) for discussions and editing our manuscript.

Supported by research grants from the Japan Agency for Medical Research and Development (AMED), the Ministry of Health, Labor and Welfare, and Japan (18ek0109282h0002 to TI); Grants-in-Aid for Scientific Research, Japan Society for the Promotion of Science (H26-26462674 to KT; 16H06269 and 16KK0193 to KF); and National Hospital Organization Network Research Fund (H30-NHO-Sensory Organs-03 to KF and KT). KF is supported by Foundation Fighting Blindness, USA and Great Britain Sasakawa Foundation Butterfield Awards, UK. The authors have no proprietary or commercial interest in any materials discussed in this article. GA is supported by a Fight for Sight (UK) Early career investigator award, NIHR-BRC at Moorfields Eye Hospital and the UCL Institute of Ophthalmology, NIHR-BRC at Great Ormond Street Hospital and UCL Institute of Child Health, and Great Britain Sasakawa Foundation Butterfield Award, UK. NP is supported by the the NIHR-BRC at Moorfields Eye Hospital and the UCL Institute of Ophthalmology.

Disclosure: **S. Kameya**, None; **K. Fujinami**, None; **S. Ueno**, None; **T. Hayashi**, None; **K. Kuniyoshi**, None; **R. Ideta**, None; **S. Kikuchi**, None; **D. Kubota**, None; **K. Yoshitake**, None; **S. Katagiri**, None; **H. Sakuramoto**, None; **T. Kominami**, None; **H. Terasaki**, None; **L. Yang**, None; **Y. Fujinami-Yokokawa**, None; **X. Liu**, None; **G. Arno**, None; **N. Pontikos**, None; **Y. Miyake**, None; **T. Iwata**, None; **K. Tsunoda**, None

References

1. Van Ghelue M, Eriksen HL, Ponjavic V, et al. Autosomal dominant cone-rod dystrophy due to a missense mutation (R838C) in the guanylate cyclase 2D gene (GUCY2D) with preserved rod function in one branch of the family. *Ophthalmic Genet*. 2000;21:197–209.
2. Downes SM, Payne AM, Kelsell RE, et al. Autosomal dominant cone-rod dystrophy with mutations in the guanylate cyclase 2D gene encoding retinal guanylate cyclase-1. *Arch Ophthalmol*. 2001;119:1667–1673.
3. Gregory-Evans K, Kelsell RE, Gregory-Evans CY, et al. Autosomal dominant cone-rod retinal dystrophy (CORD6) from heterozygous mutation of GUCY2D, which encodes retinal guanylate cyclase. *Ophthalmology*. 2000;107:55–61.
4. Ito S, Nakamura M, Nuno Y, Ohnishi Y, Nishida T, Miyake Y. Novel complex GUCY2D mutation in Japanese family with cone-rod dystrophy. *Invest Ophthalmol Vis Sci*. 2004;45:1480–1485.
5. Payne AM, Downes SM, Bessant DA, et al. A mutation in guanylate cyclase activator 1A (GUCA1A) in an autosomal dominant cone dystrophy pedigree mapping to a new locus on chromosome 6p21.1. *Hum Mol Genet*. 1998;7:273–277.
6. Jiang L, Wheaton D, Bereta G, et al. A novel GCAP1(N104K) mutation in EF-hand 3 (EF3) linked to autosomal dominant cone dystrophy. *Vision Res*. 2008;48:2425–2432.
7. Manes G, Mamouni S, Herald E, et al. Cone dystrophy or macular dystrophy associated with novel autosomal dominant GUCA1A mutations. *Mol Vis*. 2017;23:198–209.
8. Downes SM, Holder GE, Fitzke FW, et al. Autosomal dominant cone and cone-rod dystrophy with mutations in the guanylate cyclase activator 1A gene-encoding guanylate cyclase activating protein-1. *Arch Ophthalmol*. 2001;119:96–105.
9. Freund CL, Gregory-Evans CY, Furukawa T, et al. Cone-rod dystrophy due to mutations in a novel photoreceptor-specific homeobox gene (CRX) essential for maintenance of the photoreceptor. *Cell*. 1997;91:543–553.
10. Kitiratschky VB, Nagy D, Zabel T, et al. Cone and cone-rod dystrophy segregating in the same pedigree due to the same

novel CRX gene mutation. *Br J Ophthalmol*. 2008;92:1086–1091.

11. Michaelides M, Holder GE, Hunt DM, Fitzke FW, Bird AC, Moore AT. A detailed study of the phenotype of an autosomal dominant cone-rod dystrophy (CORD7) associated with mutation in the gene for RIM1. *Br J Ophthalmol*. 2005;89:198–206.
12. Pras E, Abu A, Rotenstreich Y, et al. Cone-rod dystrophy and a frameshift mutation in the PROM1 gene. *Mol Vis*. 2009;15:1709–1716.
13. Michaelides M, Gaillard MC, Escher P, et al. The PROM1 mutation p.R373C causes an autosomal dominant bull's eye maculopathy associated with rod, rod-cone, and macular dystrophy. *Invest Ophthalmol Vis Sci*. 2010;51:4771–4780.
14. Nakazawa M, Naoi N, Wada Y, et al. Autosomal dominant cone-rod dystrophy associated with a Val200Glu mutation of the peripherin/RDS gene. *Retina*. 1996;16:405–410.
15. Renner AB, Fiebig BS, Weber BH, et al. Phenotypic variability and long-term follow-up of patients with known and novel PRPH2/RDS gene mutations. *Am J Ophthalmol*. 2009;147:518–530.
16. Fishman GA, Stone EM, Grover S, Derlacki DJ, Haines HL, Hockey RR. Variation of clinical expression in patients with Stargardt dystrophy and sequence variations in the ABCR gene. *Arch Ophthalmol*. 1999;117:504–510.
17. Fujinami K, Sergouniotis PI, Davidson AE, et al. Clinical and molecular analysis of Stargardt disease with preserved foveal structure and function. *Am J Ophthalmol*. 2013;156:487–501.
18. Westeneng-van Haaften SC, Boon CJ, Cremers FP, Hoefsloot LH, den Hollander AI, Hoyng CB. Clinical and genetic characteristics of late-onset Stargardt's disease. *Ophthalmology*. 2012;119:1199–1210.
19. Klevering BJ, Blankenagel A, Maugeri A, Cremers FP, Hoyng CB, Rohrschneider K. Phenotypic spectrum of autosomal recessive cone-rod dystrophies caused by mutations in the ABCA4 (ABCR) gene. *Invest Ophthalmol Vis Sci*. 2002;43:1980–1985.
20. Wissinger B, Dangel S, Jagle H, et al. Cone dystrophy with supernormal rod response is strictly associated with mutations in KCNV2. *Invest Ophthalmol Vis Sci*. 2008;49:751–757.
21. Robson AG, Webster AR, Michaelides M, et al. "Cone dystrophy with supernormal rod electroretinogram": a comprehensive genotype/phenotype study including fundus autofluorescence and extensive electrophysiology. *Retina*. 2010;30:51–62.
22. Fujinami K, Tsunoda K, Nakamura N, et al. Molecular characteristics of four Japanese cases with KCNV2 retinopathy: report of novel disease-causing variants. *Mol Vis*. 2013;19:1580–1590.
23. Ebenezer ND, Michaelides M, Jenkins SA, et al. Identification of novel RPGR ORF15 mutations in X-linked progressive cone-rod dystrophy (XLCORD) families. *Invest Ophthalmol Vis Sci*. 2005;46:1891–1898.
24. Thiadens AA, Soerjoesing GG, Florijn RJ, et al. Clinical course of cone dystrophy caused by mutations in the RPGR gene. *Graefes Arch Clin Exp Ophthalmol*. 2011;249:1527–1535.
25. Ito S, Nakamura M, Ohnishi Y, Miyake Y. Autosomal dominant cone-rod dystrophy with R838H and R838C mutations in the GUCY2D gene in Japanese patients. *Jpn J Ophthalmol*. 2004;48:228–235.
26. Kikuchi S, Kameya S, Gocho K, et al. Cone dystrophy in patient with homozygous RP1L1 mutation. *Biomed Res Int*. 2015;2015:545243.
27. Kominami A, Ueno S, Kominami T, et al. Case of cone dystrophy with normal fundus appearance associated with biallelic POC1B variants. *Ophthalmic Genet*. 2018;39:255–262.
28. Jin X, Chen L, Wang D, Zhang Y, Chen Z, Huang H. Novel compound heterozygous mutation in the POC1B gene underlie peripheral cone dystrophy in a Chinese family. *Ophthalmic Genet*. 2018;39:300–306.
29. Roosing S, Lamers IJ, de Vrieze E, et al. Disruption of the basal body protein POC1B results in autosomal-recessive cone-rod dystrophy. *Am J Hum Genet*. 2014;95:131–142.
30. Durlu YK, Koroglu C, Tolun A. Novel recessive cone-rod dystrophy caused by POC1B mutation. *JAMA Ophthalmol*. 2014;132:1185–1191.
31. Beck BB, Phillips JB, Bartram MP, et al. Mutation of POC1B in a severe syndromic retinal ciliopathy. *Hum Mutat*. 2014;35:1153–1162.
32. Ito N, Kameya S, Gocho K, et al. Multimodal imaging of a case of peripheral cone dystrophy. *Doc Ophthalmol*. 2015;130:241–251.
33. Kato Y, Hanazono G, Fujinami K, et al. Parafoveal photoreceptor abnormalities in asymptomatic patients with RP1L1 mutations in families with occult macular dystrophy. *Invest Ophthalmol Vis Sci*. 2017;58:6020–6029.
34. Robson AG, Nilsson J, Li S, et al. ISCEV guide to visual electrodiagnostic procedures. *Doc Ophthalmol*. 2018;136:1–26.
35. Fujinami K, Kameya S, Kikuchi S, et al. Novel RP1L1 variants and genotype-photoreceptor microstructural phenotype associations in cohort of Japanese patients with occult macular dystrophy. *Invest Ophthalmol Vis Sci*. 2016;57:4837–4846.
36. Richards S, Aziz N, Bale S, et al. Standards and guidelines for the interpretation of sequence variants: a joint consensus recommendation of the American College of Medical Genetics and Genomics and the Association for Molecular Pathology. *Genet Med*. 2015;17:405–424.
37. Pearson CG, Osborn DP, Giddings TH Jr, Beales PL, Winey M. Basal body stability and ciliogenesis requires the conserved component Poc1. *J Cell Biol*. 2009;187:905–920.
38. Keller LC, Geimer S, Romijn E, Yates J III, Zamora I, Marshall WF. Molecular architecture of the centriole proteome: the conserved WD40 domain protein POC1 is required for centriole duplication and length control. *Mol Biol Cell*. 2009;20:1150–1166.
39. Venoux M, Tait X, Hames RS, Straatman KR, Woodland HR, Fry AM. Poc1A and Poc1B act together in human cells to ensure centriole integrity. *J Cell Sci*. 2013;126:163–175.
40. Zhang C, Zhang Q, Wang F, Liu Q. Knockdown of poc1b causes abnormal photoreceptor sensory cilium and vision impairment in zebrafish. *Biochem Biophys Res Commun*. 2015;465:651–657.
41. Birtel J, Eisenberger T, Gliem M, et al. Clinical and genetic characteristics of 251 consecutive patients with macular and cone/cone-rod dystrophy. *Sci Rep*. 2018;8:4824.
42. Boon CJ, Klevering BJ, den Hollander AI, et al. Clinical and genetic heterogeneity in multifocal vitelliform dystrophy. *Arch Ophthalmol*. 2007;125:1100–1106.
43. Fakin A, Robson AG, Chiang JP, et al. The effect on retinal structure and function of 15 specific ABCA4 mutations: a detailed examination of 82 hemizygous patients. *Invest Ophthalmol Vis Sci*. 2016;57:5963–5973.
44. Kondo M, Miyake Y, Kondo N, Ueno S, Takakuwa H, Terasaki H. Peripheral cone dystrophy: a variant of cone dystrophy with predominant dysfunction in the peripheral cone system. *Ophthalmology*. 2004;111:732–739.
45. Rotenstreich Y, Fishman GA, Anderson RJ. Visual acuity loss and clinical observations in a large series of patients with Stargardt disease. *Ophthalmology*. 2003;110:1151–1158.

Investigative Ophthalmology & Visual Science

46. Nakao T, Tsujikawa M, Sawa M, Gomi F, Nishida K. Foveal sparing in patients with Japanese Stargardt's disease and good visual acuity. *Jpn J Ophthalmol*. 2012;56:584–588.
47. van Huet RA, Bax NM, Westeneng-Van Haaften SC, et al. Foveal sparing in Stargardt disease. *Invest Ophthalmol Vis Sci*. 2014;55:7467–7478.
48. Duncker T, Tsang SH, Woods RL, et al. Quantitative fundus autofluorescence and optical coherence tomography in PRPH2/RDS- and ABCA4-associated disease exhibiting phenotypic overlap. *Invest Ophthalmol Vis Sci*. 2015;56:3159–3170.
49. de Laat P, Smeitink JA, Janssen MC, Keunen JE, Boon CJ. Mitochondrial retinal dystrophy associated with the m.3243A>G mutation. *Ophthalmology*. 2013;120:2684–2696.
50. Tsang SH, Burke T, Oll M, et al. Whole exome sequencing identifies CRB1 defect in an unusual maculopathy phenotype. *Ophthalmology*. 2014;121:1773–1782.
51. Sunness JS, Bressler NM, Maguire MG. Scanning laser ophthalmoscopic analysis of the pattern of visual loss in age-related geographic atrophy of the macula. *Am J Ophthalmol*. 1995;119:143–151.
52. Forte R, Querques G, Querques L, Leveziel N, Benhamou N, Souied EH. Multimodal evaluation of foveal sparing in patients with geographicatrophy due to age-related macular degeneration. *Retina*. 2013;33:482–489.
53. Steinberg JS, Fleckenstein M, Holz FG, Schmitz-Valckenberg S. Foveal sparing of reticular drusen in eyes with early and intermediate age-related macular degeneration. Invest *Ophthalmol Vis Sci*. 2015;56:4267–4274.
54. Querques G, Kamami-Levy C, Georges A, et al. Adaptive optics imaging of foveal sparing in geographic atrophy secondary to age-related macular degeneration. *Retina*. 2016;36:247–254.
55. Chucair AJ, Rotstein NP, Sangiovanni JP, During A, Chew EY, Politi LE. Lutein and zeaxanthin protect photoreceptors from apoptosis induced by oxidative stress: relation with docosahexaenoic acid. *Invest Ophthalmol Vis Sci*. 2007;48:5168–5177.
56. Aleman TS, Cideciyan AV, Windsor EA, et al. Macular pigment and lutein supplementation in ABCA4-associated retinal degenerations. *Invest Ophthalmol Vis Sci*. 2007;48:1319–1329.
57. Curcio CA, Sloan KR Jr, Packer O, Hendrickson AE, Kalina RE. Distribution of cones in human and monkey retina: individual variability and radial asymmetry. *Science*. 1987;236:579–582.
58. Wang JS, Kefalov VJ. The cone-specific visual cycle. *Prog Retin Eye Res*. 2011;30:115–128.
59. Curcio CA, Millican CL, Allen KA, Kalina RE. Aging of the human photoreceptor mosaic: evidence for selective vulnerability of rods in central retina. *Invest Ophthalmol Vis Sci*. 1993;34:3278–3296.
60. Curcio CA, Allen KA, Sloan KR, et al. Distribution and morphology of human cone photoreceptors stained with anti-blue opsin. *J Comp Neurol*. 1991;312:610–624.
61. Okano K, Maeda A, Chen Y, et al. Retinal cone and rod photoreceptor cells exhibit differential susceptibility to light-induced damage. *J Neurochem*. 2012;121:146–156.
62. Snodderly DM, Sandstrom MM, Leung IY, Zucker CL, Neuringer M. Retinal pigment epithelial cell distribution in central retina of rhesus monkeys. *Invest Ophthalmol Vis Sci*. 2002;43:2815–2818.
63. Leveillard T, Mohand-Said S, Lorentz O, et al. Identification and characterization of rod-derived cone viability factor. *Nat Genet*. 2004;36:755–759.
64. Tsunoda K, Usui T, Hatase T, et al. Clinical characteristics of occult macular dystrophy in family with mutation of Rp111 gene. *Retina*. 2012;32:1135–1147.
65. Miyake Y, Tsunoda K. Occult macular dystrophy. *Jpn J Ophthalmol*. 2015;59:71–80.
66. Hong HK, Ferrell RE, Gorin MB. Clinical diversity and chromosomal localization of X-linked cone dystrophy (COD1). *Am J Hum Genet*. 1994;55:1173–1181.
67. Jin ZB, Liu XQ, Hayakawa M, Murakami A, Nao-i N. Mutational analysis of RPGR and RP2 genes in Japanese patients with retinitis pigmentosa: identification of four mutations. *Mol Vis*. 2006;12:1167–1174.
68. Tee JJ, Smith AJ, Hardcastle AJ, Michaelides M. RPGR-associated retinopathy: clinical features, molecular genetics, animal models and therapeutic options. *Br J Ophthalmol*. 2016;100:1022–1027.
69. Gerber S, Perrault I, Hanein S, et al. Complete exon-intron structure of the RPGR-interacting protein (RPGRIP1) gene allows the identification of mutations underlying Leber congenital amaurosis. *Eur J Hum Genet*. 2001;9:561–571.
70. Patil H, Tserentsoodol N, Saha A, Hao Y, Webb M, Ferreira PA. Selective loss of RPGRIP1-dependent ciliary targeting of NPHP4, RPGR and SDCCAG8 underlies the degeneration of photoreceptor neurons. *Cell Death Dis*. 2012;3:e355.
71. Huang H, Wang Y, Chen H, et al. Targeted next generation sequencing identified novel mutations in RPGRIP1 associated with both retinitis pigmentosa and Leber's congenital amaurosis in unrelated Chinese patients. *Oncotarget*. 2017;8:35176–35183.
72. Bowne SJ, Daiger SP, Hims MM, et al. Mutations in the RP1 gene causing autosomal dominant retinitis pigmentosa. *Hum Mol Genet*. 1999;8:2121–2128.
73. Berson EL, Grimsby JL, Adams SM, et al. Clinical features and mutations in patients with dominant retinitis pigmentosa-1 (RP1). *Invest Ophthalmol Vis Sci*. 2001;42:2217–2224.
74. Jacobson SG, Cideciyan AV, Iannaccone A, et al. Disease expression of RP1 mutations causing autosomal dominant retinitis pigmentosa. *Invest Ophthalmol Vis Sci*. 2000;41:1898–1908.
75. den Hollander AI, Koenekoop RK, Yzer S, et al. Mutations in the CEP290 (NPHP6) gene are a frequent cause of Leber congenital amaurosis. *Am J Hum Genet*. 2006;79:556–561.
76. Sheck L, Davies WIL, Moradi P, et al. Leber congenital amaurosis associated with mutations in CEP290, clinical phenotype, and natural history in preparation for trials of novel therapies. *Ophthalmology*. 2018;125:894–903.
77. Ueno S, Nakanishi A, Kominami T, et al. *In vivo* imaging of a cone mosaic in a patient with achromatopsia associated with a GNAT2 variant. *Jpn J Ophthalmol*. 2017;61:92–98.
78. Ueno S, Nakanishi A, Sayo A, et al. Differences in ocular findings in two siblings: one with complete and other with incomplete achromatopsia. *Doc Ophthalmol*. 2017;134:141–147.

Appendix

Members of the Japan Eye Genetics Consortium

Atsushi Mizota,[1] Kei Shinoda,[1,2] Natsuko Nakamura,[3] Kei Mizobuchi,[4] Toshihide Nishimura,[5] Yoshihide Hayashizaki,[6] Mineo Kondo,[7] Nobuhiro Shimozawa,[8] Masayuki Horiguchi,[9] Shuichi Yamamoto,[10] Manami Kuze,[11] Nobuhisa Naoi,[12] Shigeki Machida,[13] Yoshiaki Shimada,[14] Makoto Nakamura,[15] Takashi Fujikado,[16] Hotta Yoshihiro,[17] Masayo Takahashi,[18] Kiyofumi Mochizuki,[19] Akira Murakami,[20] Hiroyuki Kondo,[21] Susumu Ishida,[22] Mitsuru Nakazawa,[23] Tetsuhisa Hatase,[24] Tatsuo Matsunaga,[25] Akiko Maeda,[18] Kosuke Noda,[22] Atsuhiro Tanikawa,[9] Syuji Yamamoto,[26] Hiroyuki Yamamoto,[26] Makoto Araie,[27] Makoto Aihara,[3] Toru Nakazawa,[28] Tetsuju Sekiryu,[29] Kenji

Kashiwagi,[30] Kenjiro Kosaki,[31] Carninci Piero,[32] Takeo Fukuchi,[33] Atsushi Hayashi,[34] Katsuhiro Hosono,[17] Keisuke Mori,[35] Kouji Tanaka,[36] Kouiti Furuya,[37] Keiichirou Suzuki,[37] Ryo Kohata,[3] Yasuo Yanagi,[38] Yuriko Minegishi,[39] Daisuke Iejima,[39] Akiko Suga,[39] Brian P. Rossmiller,[39] Yang Pan,[39] Tomoko Oshima,[39] Mao Nakayama,[39] Megumi Yamamoto,[39] Naoko Minematsu,[39] Daisuke Mori,[40] Yusuke Kijima,[40] Go Mawatari,[12] Kentaro Kurata,[17] Norihiro Yamada,[41] Masayoshi Itoh,[6] Hideya Kawaji,[6] and Yasuhiro Murakawa[42]

[1]Department of Ophthalmology, Teikyo University, Tokyo, Japan
[2]Department of Ophthalmology, Saitama Medical University, Saitama, Japan
[3]Department of Ophthalmology, The University of Tokyo, Tokyo, Japan
[4]Department of Ophthalmology, Kindai University Faculty of Medicine, Osaka, Japan
[5]Department of Translational Medicine Informatics, St. Marianna University School of Medicine, Kawasaki, Japan
[6]RIKEN Preventive Medicine and Diagnosis Innovation Program, Wako, Japan
[7]Department of Ophthalmology, Mie University Graduate School of Medicine, Mie, Japan
[8]National Institutes of Biomedical Innovation, Health and Nutrition, Tsukuba, Japan
[9]Department of Ophthalmology, Fujita Health University School of Medicine, Toyoake, Japan
[10]Department of Ophthalmology and Visual Science, Chiba University Graduate School of Medicine, Chiba, Japan
[11]Department of Ophthalmology, Matsusaka Central General Hospital, Matsusaka, Japan
[12]Department of Ophthalmology, University of Miyazaki, Miyazaki, Japan
[13]Saitama Medical Center, Dokkyo Medical University, Koshigaya, Saitama, Japan
[14]Fujita Health University, Banbuntane Hospital, Nagoya, Japan
[15]Department of Ophthalmology, Kobe University Hospital, Kobe, Japan
[16]Osaka University Medical School, Suita, Japan
[17]Hamamatsu University School of Medicine, Hamamatsu, Japan
[18]Riken Center for Developmental Biology, Kobe, Hyogo, Japan
[19]Department of Ophthalmology Gifu University Graduate School of Medicine, Gifu, Japan
[20]Department of Ophthalmology, Juntendo University Faculty of Medicine, Tokyo, Japan.
[21]Department of Ophthalmology, University of Occupational and Environmental Health, Kitakyuusyuu, Japan
[22]Laboratory of Ocular Cell Biology and Visual Science, Department of Ophthalmology, Faculty of Medicine and Graduate School of Medicine, Hokkaido University, Sapporo, Hokkaido, Japan
[23]Hirosaki University Graduate School of Medicine, Hirosaki-shi, Japan
[24]Graduate School of Medical and Dental Sciences, Niigata University, Niigata, Japan
[25]Division of Hearing and Balance Research, National Institute of Sensory Organs, National Hospital Organization, Tokyo Medical Center, Tokyo, Japan
[26]Hitoshi Ophthalmology Clinic, Nishinomiya, Japan
[27]Kanto Central Hospital of the Mutual Aid Association of Public School Teachers, Tokyo, Japan
[28]Department of Ophthalmology, Graduate School of Medicine, Tohoku University, Sendai, Japan
[29]Department of Ophthalmology, Fukushima Medical University School of Medicine, Fukushima, Japan
[30]Department of Ophthalmology, University of Yamanashi, Yamanashi, Japan
[31]Center for Medical Genetics, Keio University School of Medicine, Tokyo, Japan
[32]Division of Genomic Technologies, Laboratory for Transcriptome Technology, RIKEN Center for Integrative Medical Sciences, Yokohama, Japan
[33]Division of Ophthalmology and Visual Science, Graduate School of Medical and Dental Sciences, Niigata University, Niigata, Japan
[34]Department of Ophthalmology, Graduate School of Medicine and Pharmaceutical Sciences, University of Toyama, Toyama, Japan
[35]Department of Ophthalmology, International University of Health and Welfare, Nasu-shiobara, Japan
[36]Department of Ophthalmology, Nihon University Hospital, Tokyo, Japan
[37]Institute for Advanced Co-Creation Studies, Osaka University, Suita, Japan
[38]Department of Ophthalmology, Asahikawa Medical University, Asahikawa, Japan
[39]Division of Molecular and Cellular Biology, National Institute of Sensory Organs, National Hospital Organization Tokyo Medical Center, Tokyo, Japan
[40]Graduate School of Agricultural and Life Sciences, The University of Tokyo, Japan
[41]Department of Ophthalmology, Saitama Medical University, Saitama, Japan
[42]RIKEN Preventive Medicine and Diagnosis Innovation Program, Yokohama, Japan

Investigative Ophthalmology & Visual Science